The 7th International Supercritical CO_2 Power Cycles Symposium
February 21 – 24, 2022, San Antonio, Texas
Paper #170

Investigation of Weldment Cracking During Fabrication of a 700ºC Fired sCO2 Heater

John Shingledecker, Ph.D., FASM
Senior Technical Executive
Electric Power Research Institute
Charlotte, NC USA

Dr. Shingledecker, is a Sr. Tech. Executive in Generation research area with responsibility for Technology Innovation, strategic planning, and technical leadership of collaborative projects focused on advanced manufacturing methods and materials. His research in the high-temperature behavior of engineering materials includes over 200 publications and multiple awards for technology transfer.

John Siefert, Ph.D.
Program Manager, Materials & Repair
Electric Power Research Institute (EPRI)
Charlotte, NC USA

Dr. Siefert, is the Program Manager of EPRI's Materials & Repair Program. His experiences in welding research are diverse and include the examination and behavior of a wide range of materials including creep strength enhanced ferritic materials, advanced stainless steels, nickel-base alloys, and dissimilar metal welds. He was the recipient of the prestigious American Welding Society Professor Koichi Masubuchi Award for his overall contribution to the scientific community in the topic of materials and welding. He has authored more than 150 manuscripts.

Tapasvi Lolla, Ph.D.
Technical Leader
Electric Power Research Institute (EPRI)
Charlotte, NC USA

Dr. Lolla, is an Engineer/Scientist III in the Fossil Materials and Repair R&D program at the EPRI. He is involved in improving the understanding of damage evolution in powerplant components using advanced characterization techniques including electron microscopy. His research includes lifing of advanced stainless components, failure analysis, and developing welding guidelines. He has more than 20 peer reviewed publications.

Matthew Hauth, P.E.
Engineering Manager
Optimus Engineered Products Group
Tulsa, OK USA

Mr. Hauth is the Engineering Manager for Optimus Engineered Products and Chanute Manufacturing, both of which are units of Optimus Industries. He is responsible for ASME Section I and Section VIII, Div. 1 Code design, thermal performance rating of firetube boilers, and general piping and structural design for their equipment. He brings over 10 years of heat exchanger rating and design experience holds a Bachelor of Science in Mechanical Engineering from the University of Tulsa.

Mark Stevens
Gas Technology Institute (GTI)
Des Plaines, IL USA

Mr. Stevens is an institute Engineering at GTI leading the project engineering group in Energy Supply & Conversion providing requirements for component and system development and testing tasks, financial and schedule performance planning, tracking, and forecasting and technical support to procurement and supplier management. He is leading major equipment procurement and installation activities for the DOE sponsored STEP Program

Trenton Cook
Research Engineer
Southwest Research Institute
San Antonio, TX

Mr. Cook is a Research Engineer at Southwest Research Institute. A 2015 graduate of Texas A&M University with a B.S. in Aerospace Engineering, he currently leads the piping system design for the development of a supercritical carbon dioxide power cycle test facility. He assists in a variety of design roles for equipment specification and power cycle design. He provides technical support for a variety of machinery design activities, such as mechanical, thermal, and acoustic/pulsation analyses of fluid machinery piping systems.

ABSTRACT

The U.S. DOE Supercritical Transformational Electric Power Project (STEP Demo) is constructing a multi-user facility as a 10MW electric advanced pilot project to advance the development and deployment of supercritical carbon dioxide (sCO_2) power cycles. A key component of the overall facility is the gas-fired heater which is designed to enable sCO2 cycle conditions of 276 bar (4000 psig) at >700°C. The demanding temperature and pressure conditions are enabled by using INCONEL® alloy 740H® (UNS N07740) for the construction of the high-temperature heater coil. Over 1,600 welds of varying configuration were successfully made in alloy 740H to produce this component in the largest known world-wide application of an age-hardenabable nickel-based alloy in an ASME code compliant construction. After post-weld heat-treatment of the coil assembly, cracking was identified in a small percentage of tube butt welds. A detailed metallurgical investigation was undertaken on a population of samples removed from the heater to determine the failure mechanism. A comprehensive characterization of the cracking involving non-destructive evaluation methods and advanced microscopy methods indicated stress relaxation cracking (also referred to as stress relief cracking or strain age cracking) during post-weld heat-treatment was the operative failure mechanism. This paper will discuss the metallurgical evidence for this finding, the likely contributing factors to the cracking, inspection considerations, and ongoing research to develop improved guidance for future applications.

INTRODUCTION & BACKGROUND

Project Background

The U.S. Department of Energy (DOE) Supercritical Transformational Electric Power Project (STEP Demo) is funding a project through GTI, and partners, Southwest Research Institute (SwRI) and GE Research (GE-R) to construct a 10MW Pilot Plant Test Facility that will provide valuable insight into the ability of sCO2 power cycles to provide efficient power to the grid. The design of this facility required close coordination between numerous equipment suppliers to provide custom, and often first-of-its-kind, major equipment components (turbomachinery, recuperators, compressors, etc.) to satisfy the extreme STEP process requirements. The project will verify, at the 10MW electric scale, the performance of major components in both a simple cycle and Recompression Closed Brayton Cycle (RCBC) configurations with a turbine inlet temperature >700°C [2]. The heat for future commercial sCO2 applications may come from a variety of sources including fossil fuels, concentrating solar power, nuclear, waste heat, or geothermal. Specific to the STEP program, a gas fired primary heater was designed and fabricated from 2018 to 2020 and installed in early 2021 to meet the facility requirements. Other STEP Project equipment is currently being installed and the facility is scheduled to begin commissioning and testing in 2022.

Heater and High-Temperature Heater Coil Design

Optimus Industries was selected via a competitive bidding process to design and fabricate the primary fired heater. The basic design criteria for five different cycle configurations are shown in Table 1 and the resultant design, depicted in Figure 1, included the following:

- 50 MW_{th} natural gas fired heater with sCO2 as working fluid
- Maximum fluid outlet conditions of: 715°C and 255 bar at 100 kg/sec
- Designed to meet ASME B&PV Code and all applicable emissions per state and local requirements

As shown in the 2-D cut-away in Figure 1, the heater was designed with ten main sections to be fabricated and shipped to site for final assembly. The heater coil module (Section A45) is the critical heat-transfer component after the burner and combustion sections for heating the sCO2 to the desired conditions. Although this section was built in a manner similar to heat recovery steam generators (HRSGs), the operating temperature exceeds state-of-the-art HRSGs by approximately 100°C and thus required one of the first widescale applications of an age-hardenable nickel-based alloy, INCONEL® Alloy ®740H (alloy 740H). This permitted the use of tube/pipe diameters and wall thicknesses within typical sizes for this type of fabrication. The boiler design conditions were 275.8 barg (4000 psig) and metal temperatures ranging from 607.2 to 746.1°C (1,125 to 1,375°F). The design was compliant with ASME B&PV Code Section I and in total the heater utilized ~25,000 kg (55,000 lbs) of 740H including ~6,100 m (~20,000 feet) of tubing.

Table 1. Primary Heater Design Criteria

Cycle Configuration	Qin [MW]	Pnet [MWe]	NOx [lbs/hr]	Heater Inlet		Heater Outlet		
				[bar]	[°C]	[bar]	[°C]	[kg/s]
100% Simple	21.30	6.50	0.910	212.0	319	208.0	500	95.7
40% Simple	13.47	3.58	0.510	173.6	355	171.0	500	76.2
100% RCBC	22.54	10.30	1.440*	254.1	542	250.3	715	103.1
40% RCBC	10.21	4.03	0.056	172.9	593	170.3	715	66.9
500C RCBC	21.15	7.59	1.063	254.1	355	250.3	500	116.6

**for power >8.8MWe, NOx limit is 1.54 lbs/hrs*

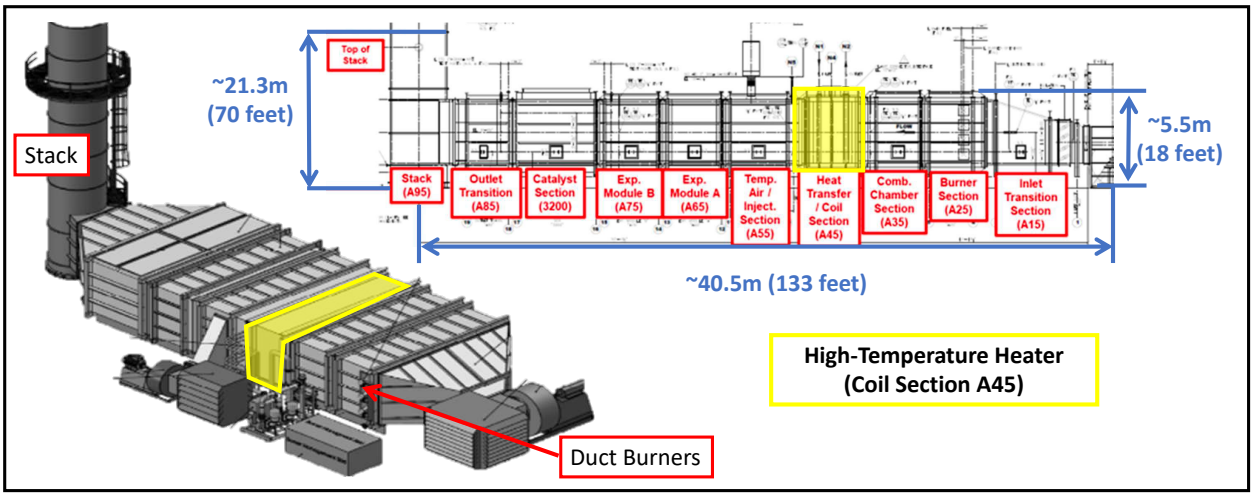

Figure 1. STEP Process Gas-Fired Heater – high temperature coil section highlighted

Some specific design features of the heater coil included [3]:

- A floating coil design to minimize thermal expansion stresses in tubes and headers
    - Cast tubesheets were used to support the coils at even intervals to allow tubes to freely slide through supports and facilitate installation
- 38.1 mm (1.5-inch) outer diameter (OD) heat-transfer tubing with varying wall thickness and spiral wound fins specially designed to control tube metal temperatures by balancing heat absorption through changing of fin height, pitch, fin material (304 and 409 stainless steel), and style throughout the coil.
- 114, 219, and 286 mm (4.5, 8.625, 11.25-inch) OD pipe headers with Grayloc™ (clamp style) connections to connect to supply and return piping for minimizing field welding

Manufacturing Experience

The alloy 740H procurement and fabrication was conducted in accordance with ASME B&PV Code Case 2702-3 [4]. Interpretation of this code case necessitated the following which had to be considered in the manufacturing development (some of these requirements are not considered for other materials which do not require an age-hardening heat-treatment after solution annealing and/or after welding):

- Welding was conducted only on solution annealed (SA) + aged material
    - Most materials procured were in the SA + aged condition so they could be directly welded including the finned tubing
    - Tubes to be used for cold-bending operations were procured in the SA condition to reduce bending loads
        - For cold-forming strains exceeding 5%, a SA + age must be performed on the entire part. Therefore, tube bending was performed on short tube lengths of SA tubes and then given a SA + aging heat-treatment before being welded into the assembly (see Figure 2a)
    - Header pipes were delivered in the SA condition to permit ease of manufacturing (e.g., cutting operations such as bore hole penetrations)

    - Later code case revisions, and in part based on feedback from projects such as this and varying interpretations of the code rules, explicitly allowed for welding in either the SA or the SA + aged condition

- All welds required an aging post-weld heat-treatment (PWHT) which could be performed locally or on the entire component
    - It was decided to weld the entire coil first, place it in a frame, and perform the PWHT of the entire assembly
    - Later, weld repairs were performed locally with ceramic heating pad blankets as is typically used in field PWHT

All welding was performed via manual gas tungsten arc welding (GTAW) with an inert gas purge (He-Ar mixture). Welding procedures were developed in accordance with Code Case 2702-3 using matching 740H filler metals for 740H to 740H as well as 740H to P-No. 8, or P-No. 43, or P-No. 45 materials. Six welders were qualified to execute thin section welding and two welders for thick section welding to the headers. Qualifications were performed in accordance with ASME B&PV Code Section IX. All welds were assessed using non-destructive examination (NDE) acceptance procedures to ASME Section V. NDE included visual inspection of root passes, liquid penetrate (PT) on finished welds, and radiographic testing (RT) on all butt welds prior to PWHT. After coil completion including PWHT, hydrostatic testing was conducted in accordance with ASME B&PV Code Section I at 1.5X design (6,000 psig). After cracking was identified in the coil, an optimized NDE procedure was implemented relying on phased array ultrasonic testing (PAUT) for 100% of tube butt welds and a second hydrostatic test at 7,299 psig. The pressure was calculated to simulate the equivalent stress ratio expected at operating temperature.

Figure 2 shows the different types of welds utilized for construction. In total, >1,600 welds were made in 740H representing the largest, to the authors' knowledge, application of an age hardenable pressure part alloy for ASME service. The general fabrication and assembly sequence involved first machining and bending (including post-bending heat-treatments) followed by welding of free-floating bends (Figure 2a and b), tube-to-header welding (Figure 2c), and heavy section welding (Figures 2d and e). To complete the assembly, the headers were aligned on one end of the assembly with the tubes aligned via the tubesheets. Then closure welds using varying radii tube bends were performed on the 'return end' of the heater as shown in Figure 3. Following NDE (visual, PT, RT), the entire assembly was placed in a heat-treatment furnace (Figure 4) with 11 thermocouples placed around the furnace to confirm the heater reached a uniform, desired temperature range of 760 to 815°C (1,400 to 1,500°F). The duration of the PWHT, after reaching temperature, was five hours.

After PWHT, the hydrostatic a pressure test was conducted, and leaks were identified in 12 tube-to-tube butt welds (11 on the return side). Figure 5a and 5b shows the typical observed leaks. A repair plan for these welds (Figure 5c-e) involved moving the tube-sheet and flexing the existing tubes to gain access, removing the entire weld and cracked area on both sides of the welds, preparing a short 'pup piece' to bridge the gap, inner diameter cleaning, rewelding and inspection, local PWHT using heating pads, and post-PWHT inspection.

Subsequent pressure test and visual inspection revealed four additional through-wall leaks (16 total). It was then decided to perform PAUT on 100% of the tube-to-tube butt welds. Additional welds were removed based on the PAUT findings, and the same repair procedure was applied. An additional hydrostatic test was successfully conducted after all repairs were completed, and the assembly was prepared for shipment to site.

Throughout this staged inspection and repair process, several welds were removed for destructive metallographic analysis to understand the failure mechanism to inform repair strategies, develop and confirm the PAUT methodology for dispositioning of indications, and provide guidance on root cause for future applications. One key early finding was clear evidence for inner diameter (ID)-initiated cracking near or at the weld root fusion line. Thus, surface inspection was found to be of limited value and a volumetric technique, in this case PAUT, was needed to inspect for sub-surface cracking. 100% PAUT inspection of all tubing joints significantly reduced the risk to conducting costly field repairs after final assembly compared to the in-shop inspection and repair approach. The PAUT procedure can serve as a basis for future field inspection to monitor structural health as the component will be subjected to thermal cycling and operation ≥700°C.

Figure 2. Types of 740H welds in STEP heater: tube-to-tube bend (a), fin butt welds tubes (b), tube-to-header welds (c), pipe-to-flange girth weld (d), and header end cap (e).

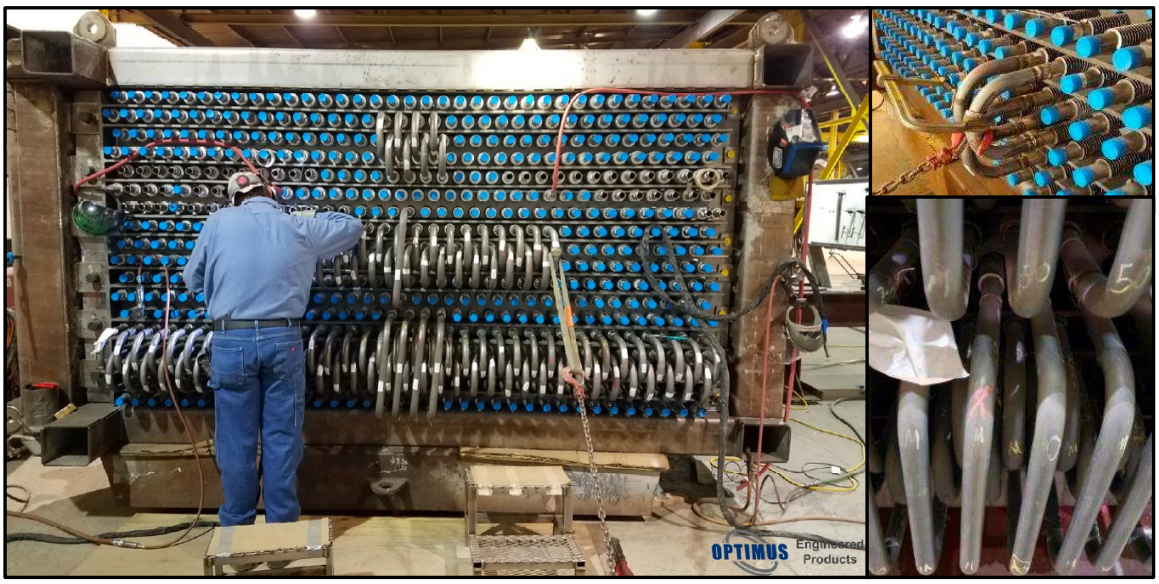

Figure 3. Final welding of the assembly on heater coil return end

Figure 4. Heater coil prior to heat treatment (insert is picture of heat-treatment furnace)

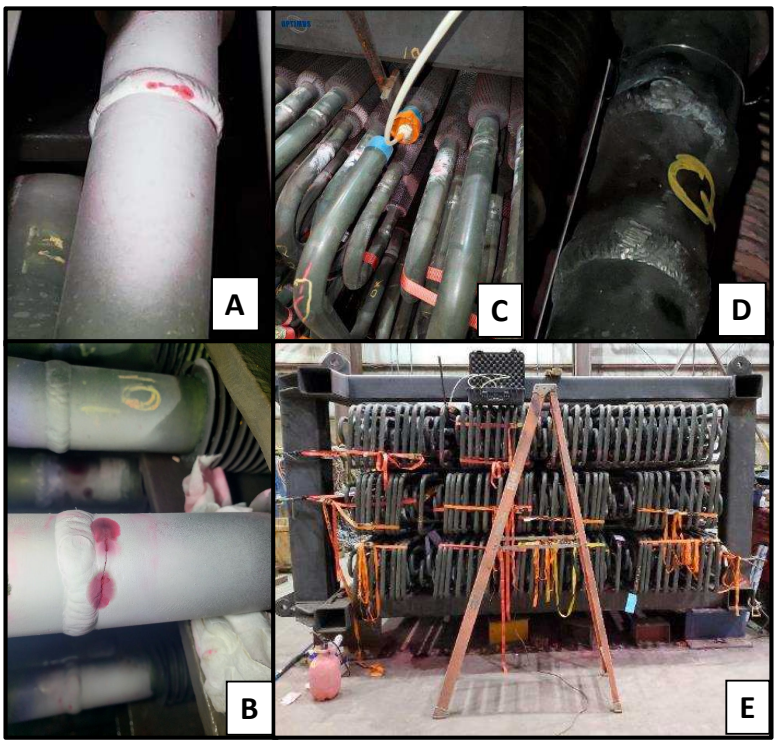

Figure 5. Cracking observed after PWHT (a and b) in 740H tube butt welds and repair procedure including removal (c), pup-piece replacement (d), and moving tubes for welder access (e)

EXPERIMENTAL PROCEDURE FOR FAILURE INVESTIGATION

EPRI was tasked with leading the investigation of cracking in the alloy 740H tube-to-tube butt welds of the STEP heater. This involved review of the fabrication documentation, welding and heat-treatment procedures, discussions with Optimus and Special Metals (the alloy manufacturer), and destructive metallographic evaluation of both cracked and uncracked samples. EPRI examined five of the original twelve cracked tubes with through-wall leaks found after the first hydro test and an additional six welds removed after PAUT NDE including three tubes with crack-like indications and three welds which did not show these same indications. The basic sectioning approach utilized is shown in Figure 6. After reviewing the provided documentation and markings on the tube, the tubes were split lengthwise being careful to avoid cutting into any suggested cracking (6a). Liquid penetrant testing (LPT) was conducted on the outer diameter (OD) and ID to determine the location and extent of the cracking (6b). Next, metallographic cross-sections were taken at the middle of the cracking and radially around the circumference (6c) including the opposite side of the tube where no cracking was identified by means of LPT. In total over 30 metallurgical mounts were prepared to support the investigation. Samples were mounted and polished using conventional methods and examined in both unetched and etched conditions using optical metallography, microhardness mapping, and scanning electron microscopy (SEM).

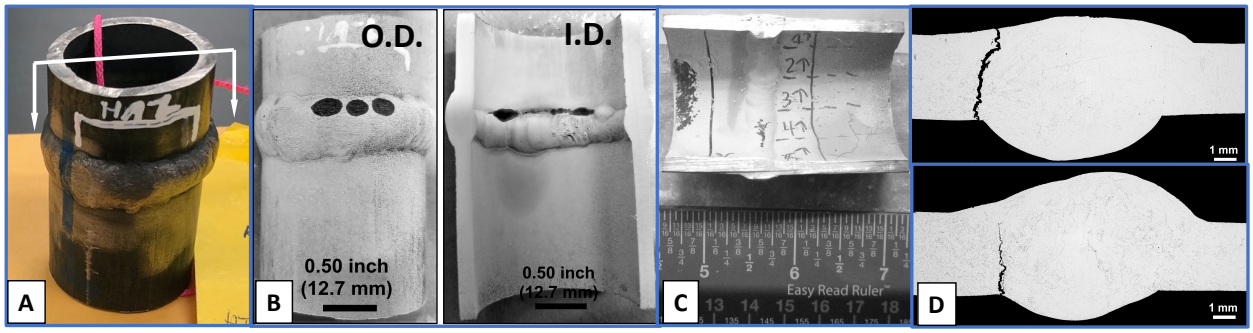

Figure 6. Tube failure investigation sectioning approach. (a) split tube lengthwise, (b) die penetrate inspection on OD and ID to identify extent of cracking, (c) removal around circumference of entire weld including areas with and without cracking, and (d) cross-sectional metallographic mounts.

RESULTS

Review of fabrication variables

>1,600 welds were made in 740H for the STEP heater. The failure rate, as established using PAUT, and association with the type of weld is given in Table 2. To explore the potential variables which may have been influencing cracking in the tube-to-tube welds, Table 3 summarizes the information on tube size and location. The weld cracking was biased towards the return end and heavier wall tubing and the return side thickness transition. Destructive evaluation confirmed that crack-like NDE indications were cracks which had not propagated through-wall. Other indications noted by PAUT but dispositioned are not reported in the table. However, a review of the data show the return end had ~3.5 times the number of reported indications compared to the header end.

Table 2. STEP 740H Heater Welding Summary

Type	Description	Cracking/NDE Indications	Total Number Fabricated	Failure Rate
Thick-wall	End Plates	0	4	0%
	Flange-to-header	0	2	0%
Thin-to-thick	Tube-to-header	0	292	0%
Dissimilar	740H to 347H	0	4	0%
Thin-to-thin	Tube-to-tube butt welds	39	1,296	3.0%
	Repairs*	0	87	0%
Total		39	1,685	2.3%

**Repairs included pup piece installations for 39 cracks/indications (2X repair welds), 3 segments removed for additional NDE verification (2X repair welds) plus 3 sacrificed welds during repairs (1X repair welds)*

Table 3. Summary of Cracking and Indications in Tube-to-tube Butt Welds

Location	Tube Thickness mm (inches)	Through-wall Cracks	PAUT NDE Identified Cracks	Total Cracks Repaired	Total Original Welds	Percent Cracked & Repaired
Return	2.67 (0.105)	1	0	1	108	0.9%
	2.67 to 3.18 (0.105 to 0.125)	5	4	9	108	8.3%
	3.94 (0.155)	3	2	5	216	2.3%
	5.59 (0.220)	2	12	14	216	6.5%
	Total	*11*	*18*	*29*	*648*	*4.5%*
Header	2.67 (0.105)	0	0	0	108	0.0%
	3.18 (0.125)	1	1	2	108	1.9%
	3.18 to 3.94 (0.125 to 0.155)	0	1	1	108	0.9%
	3.94 (0.155)	0	1	1	108	0.9%
	3.94 to 5.59 (0.155 to 0.220)	1	2	3	108	2.8%
	5.59 (0.220)	3	0	3	108	2.8%
	Total	*5*	*5*	*10*	*648*	*1.5%*
Total		***16***	***23***	***39***	***1,296***	***3.0%***

Cracking macroscopic observations

Macroscopic evaluation of through wall cracks showed variable crack locations upon visual inspection of the OD surface with cracks occurring in the weld metal, heat affected zone (HAZ) and/or fusion line (FL), and in the base metal (BM) as shown in Figure 5 (field observations) and Figure 7 (lab examination). Laboratory investigation of failed tubes confirmed variable OD crack location. However, cracking was consistently identified at the weld root FL area extending approximately 1/3 around the circumference of the tube (see Figure 7). Similar analysis on three cracked tubes identified by PAUT which did not leak showed cracking at this same ID location but without an OD-connected indication.

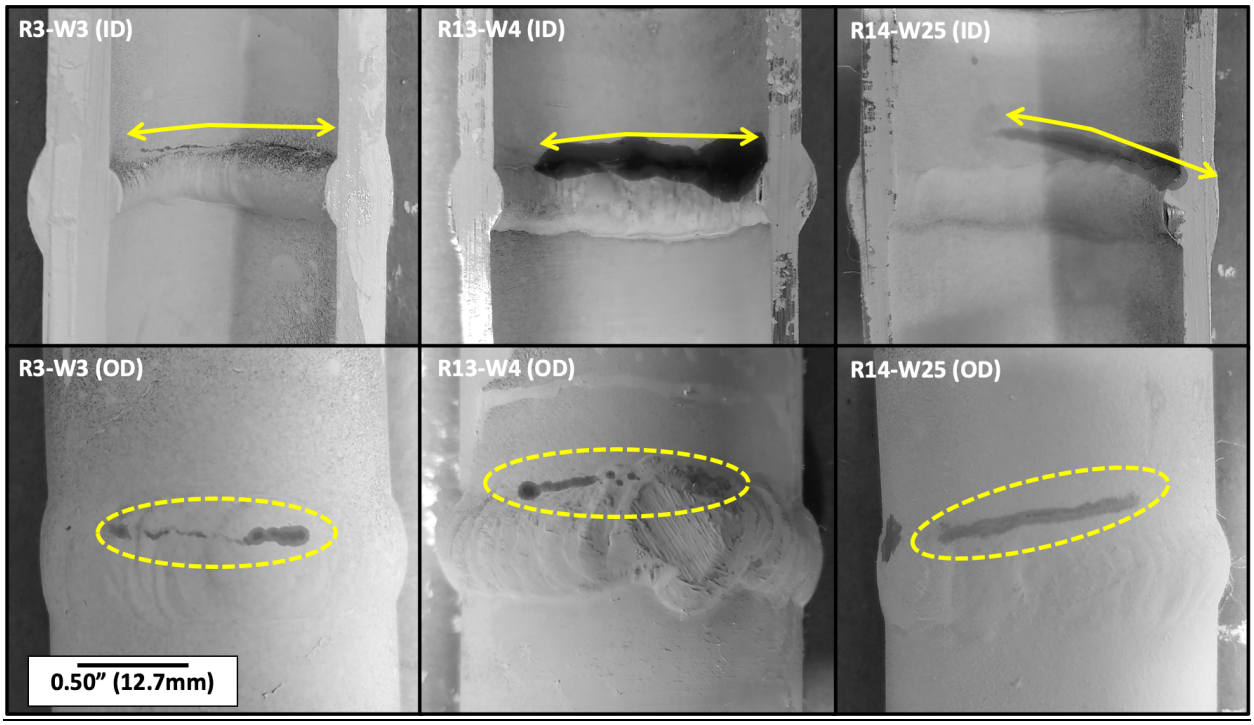

Figure 7. Die penetrate inspection showing ID fusion line cracking (top) and variable OD cracking (bottom) including weld metal (left), fusion line (center), and base metal (right). In all cases, cracks extended approximately 1/3 of circumference

Workmanship

The review of over 30 metallurgical mounts suggested that lack-of-fusion, centerline cracking, or porosity could not be solely responsible for the observed pattern of damage. Additionally, cracking was identified for multiple welders, so a specific technique or adherence to the welding procedure did not appear to be directly related to the cracking propensity. However, as shown in Figure 8, the shape of the weld was highly variable between welds and (as shown in later figures) around the weld circumference, and there was significant to excessive re-enforcement both on the ID and OD of the tubes evaluated. Some of this variability can be attributed to the accessibility of the weld and is addressed later in this report. In most cases alignment appeared to be acceptable, but there were some examples of misalignment.

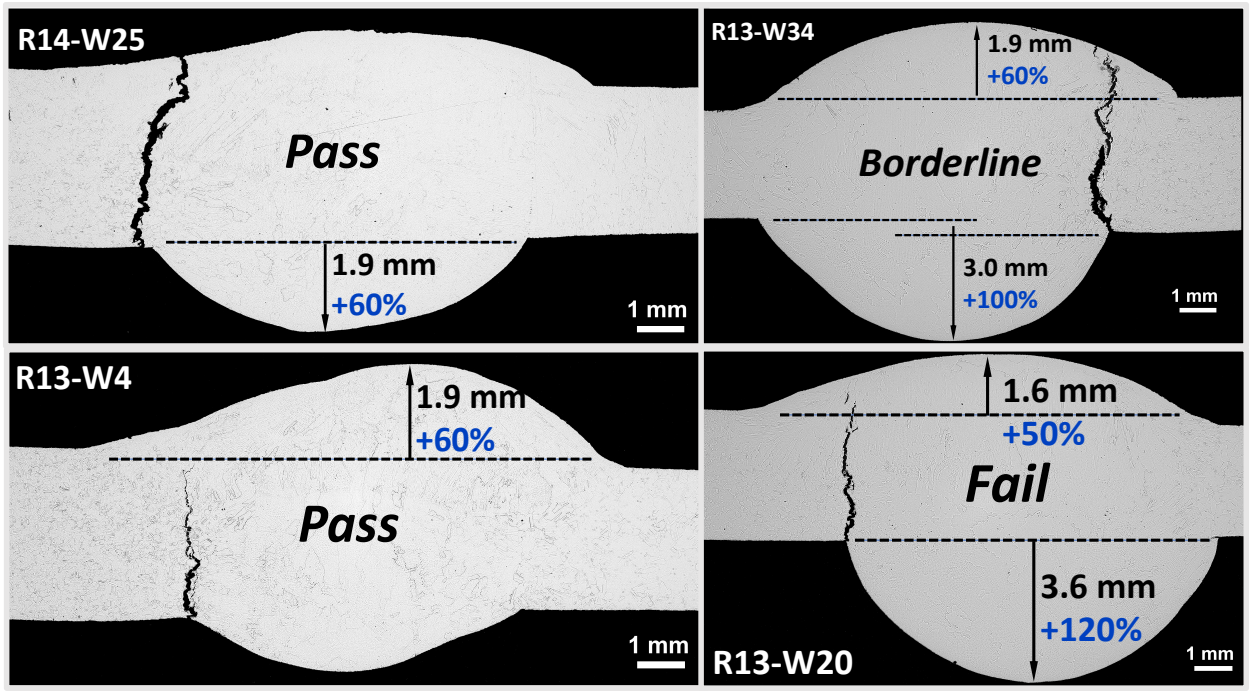

Figure 8. Examples of variable re-enforcement and weld profiles observed. Pass/fail criteria based on guidance provided by ASME B&PV Code Section I PW-35.1 [5]

Cracking morphology and progression

Inspection of the tubes and metallographic mounts taken from around the circumference of the tubes (see Figure 9 for an example on one tube) shows that cracking appears to initiate at the weld toe and propagate through the tube wall. Further evidence for crack initiation at the weld toe is shown in Figure 10 which is the center of a subsurface crack identified using PAUT. While the initiation is clearly found in the same region in all samples, crack propagation includes the HAZ, FL, weld metal, and in some cases the base metal (see Figure 7). In most cases, the eventual through-wall location appears to be dictated in-part by the variability in weld geometry as opposed to a specific microstructural constituent.

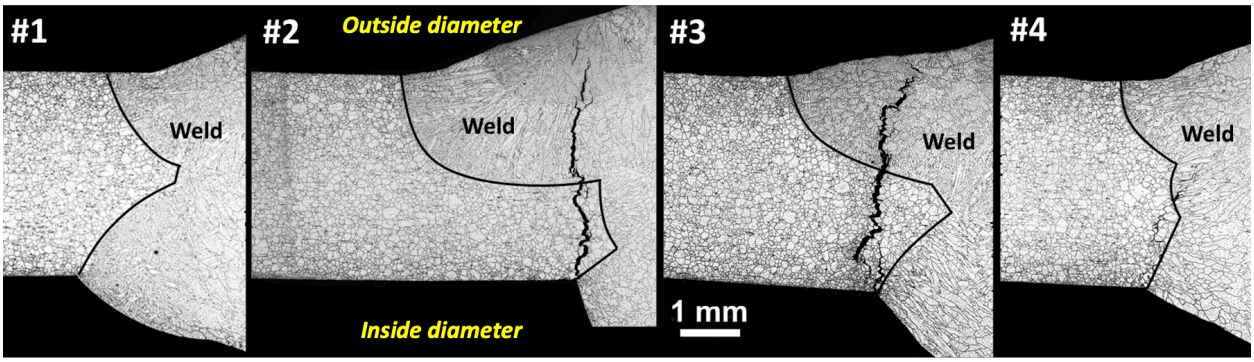

Figure 9. Cross-sectional etched micrographs for one side of a weldment (R14-W25) around the circumference showing crack initiation at the weld toe (#4), crack growth from weld toe through the HAZ and weld (#3 and #2), and no cracking (#1).

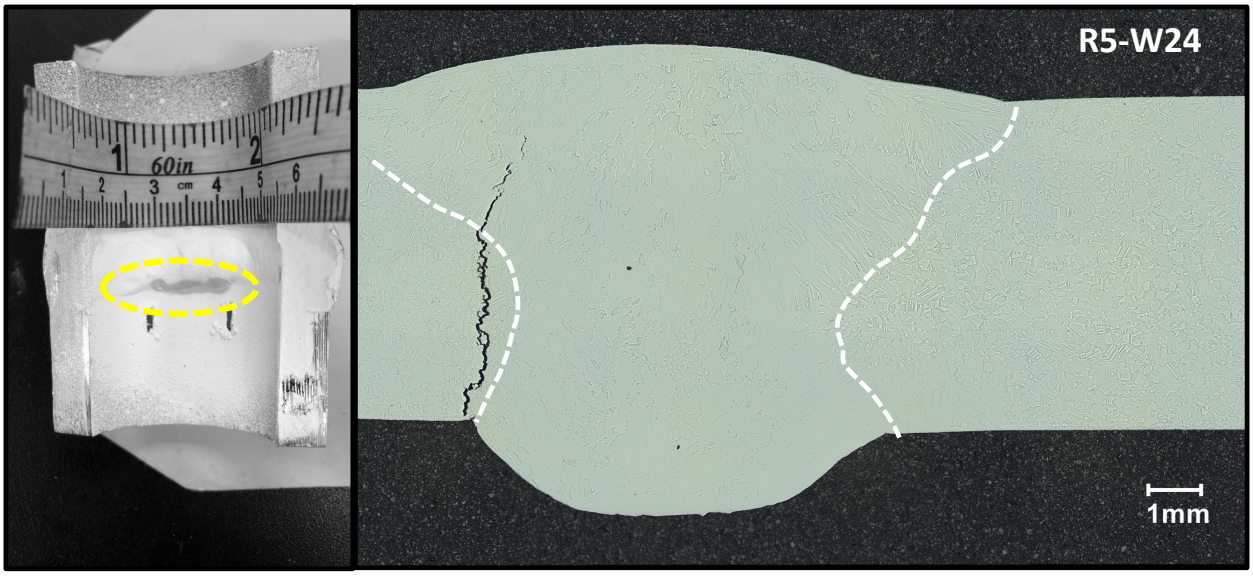

Figure 10. ID initiated cracking at weld toe (crack did not propagate through-wall)

Further investigation shows that the cracking is intergranular. Figure 11 clearly shows that both crack initiation and propagation follows grain boundaries. Furthermore, inspection of all images presented in this paper show one main crack propagating (in some cases through-wall) with minimal branching. Additional SEM evaluation of the cracking morphology, figure 12, revealed isolated grain boundary cavitation ahead of crack tips. A very thin oxide scale, figure 12, was also identified within the cracks.

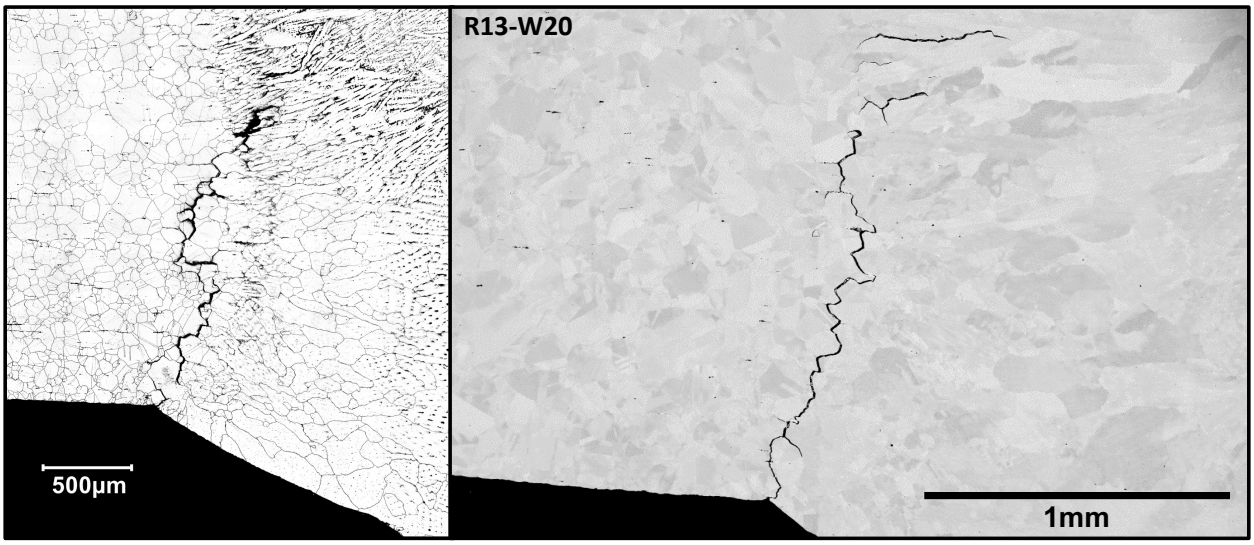

Figure 11. Etched optical (left) and SEM BSE image (right) showing intergranular crack initiation and propagation.

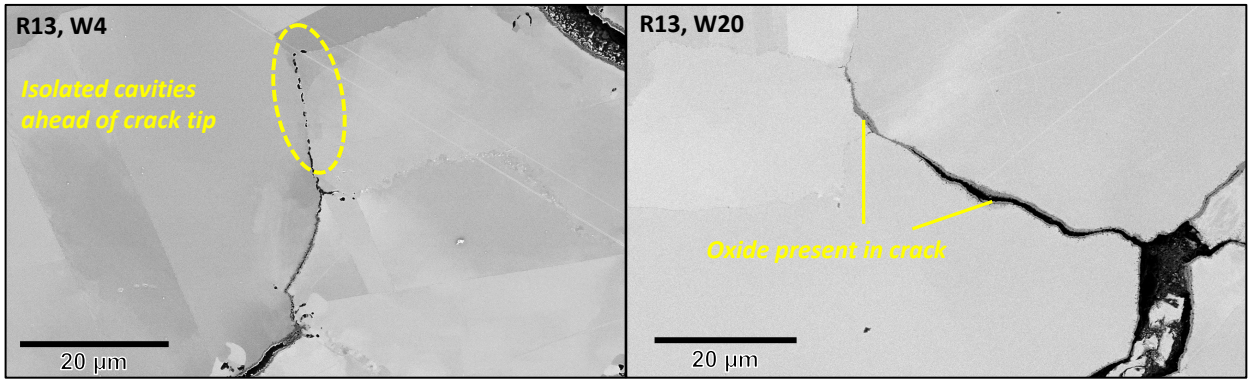

Figure 12. SEM image showing isolated cavities ahead of branching crack tips (left) and thin oxide scales in a main crack (right)

Microstructural features

To examine the general microstructure of the base metal and weldments, micro-hardness mapping was conducted on selected samples, e.g., Figure 13. In general hardness was in the range of 350 to 375 HV0.5 which is typical for alloy 740H in the aged condition. The general microstructure of the alloy 740H base metal possessed equiaxed grains with occasional carbide 'stringers'. Cracking was not associated with these stringers and no preferential orientation of cracking to other microstructural features, beyond grain boundaries, were identified, Figure 14. Grain size was not explicitly measured for all heats, but as shown in Figure 15, there were different grain sizes observed in the examined tube samples. In general, no trend was observed with cracking and grain size, and, in the case of Figure 15, cracking was found in the finer grained base metal.

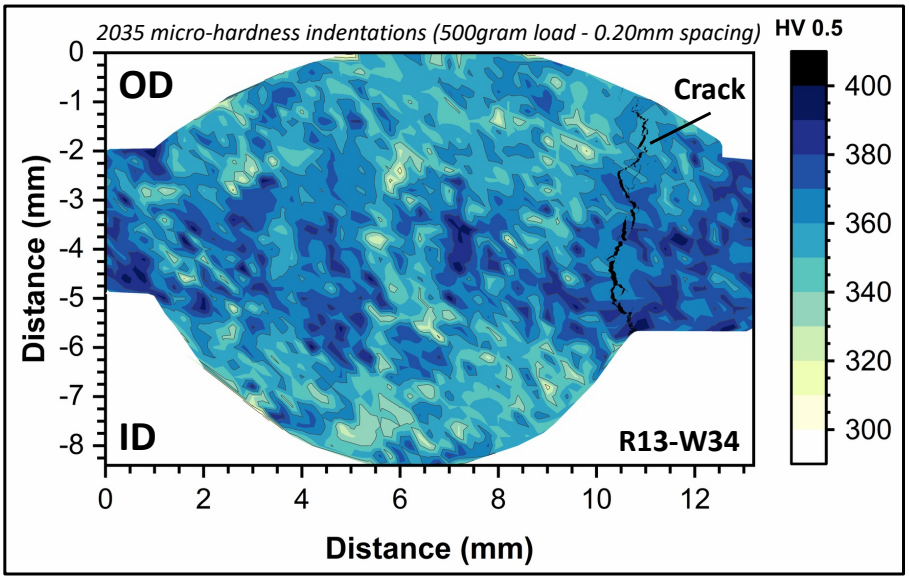

Figure 13. Hardness map showing typical and uniform hardness across the weldment

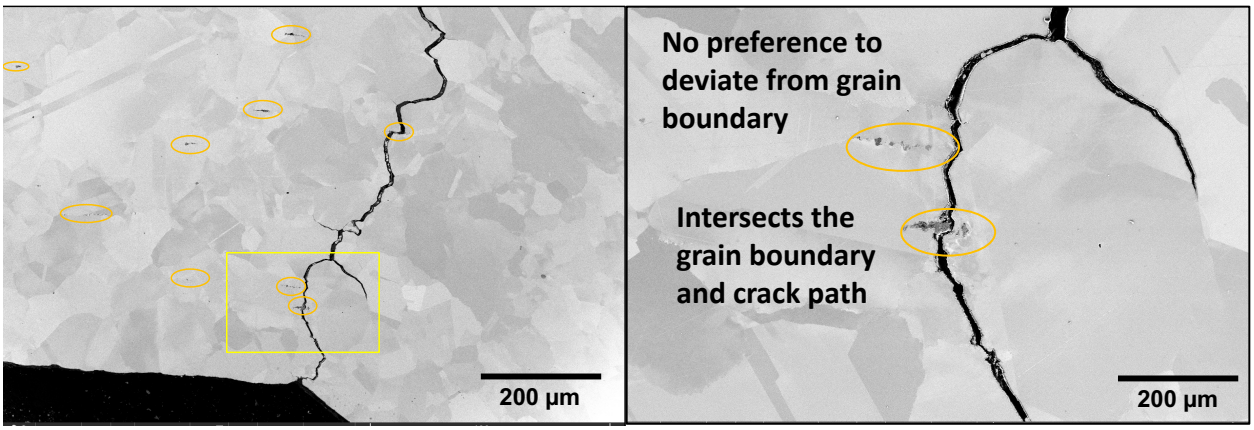

Figure 14. Lower magnification (left) SEM image and higher magnification of highlighted area (right) identifying carbide stringers throughout the matrix

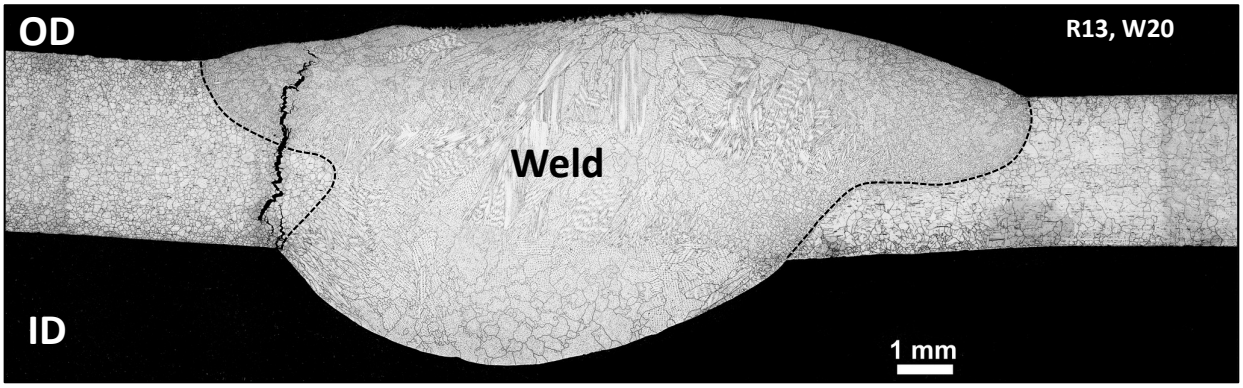

Figure 15. Etched optical image showing variation in grain size with finer grain size tubing heat (left) joined to coarser grain heat (right)

Higher resolution SEM analysis was conducted on selected samples near the ID-initiation of damage. Figure 16 shows successively higher magnification images of the same region near crack initiation and slightly removed from the crack tip. Fine spherical gamma prime (γ') precipitates are observed in the grain interiors and as expected. Inspection of the grain boundaries show coarsened grain boundary precipitates and corresponding precipitate free zones (PFZs) in the regions ahead of the crack tip. Figure 17 provides further evidence for the occurrence of PFZs near the weld root in the HAZ, and as compared to a location well-removed from the weld. The base material grain boundaries are decorated with precipitates and γ' precipitates are present to the boundary without any evidence of PFZs. Subsequent interrogation of the FL region at the weld root toe where cracking appears to be initiating showed a small region of equiaxed fine grains (Figure 18). A strong channeling contrast was also observed suggesting a highly strained region.

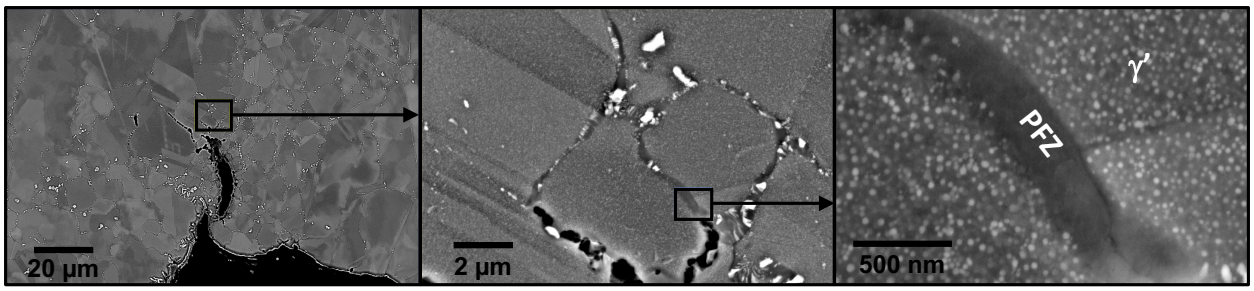

Figure 16. SEM images at 1,500X (left), 15,000X (middle), and 100,000X (right) showing microstructure ahead of possible crack initiation site including precipitate free zones (PFZ) along the grain boundaries

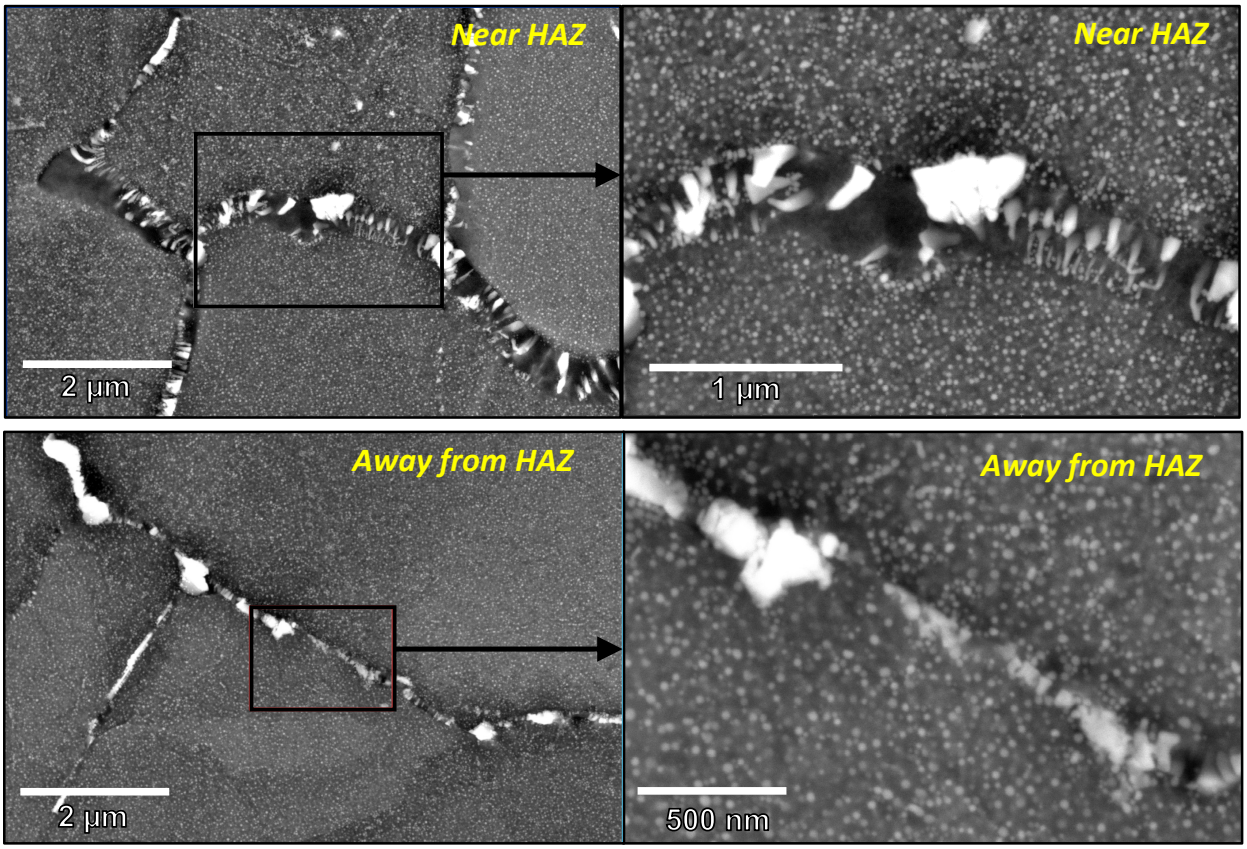

Figure 17. SEM images showing coarsened grain boundary precipitate and PFZs near the HAZ and their absence away from the HAZ

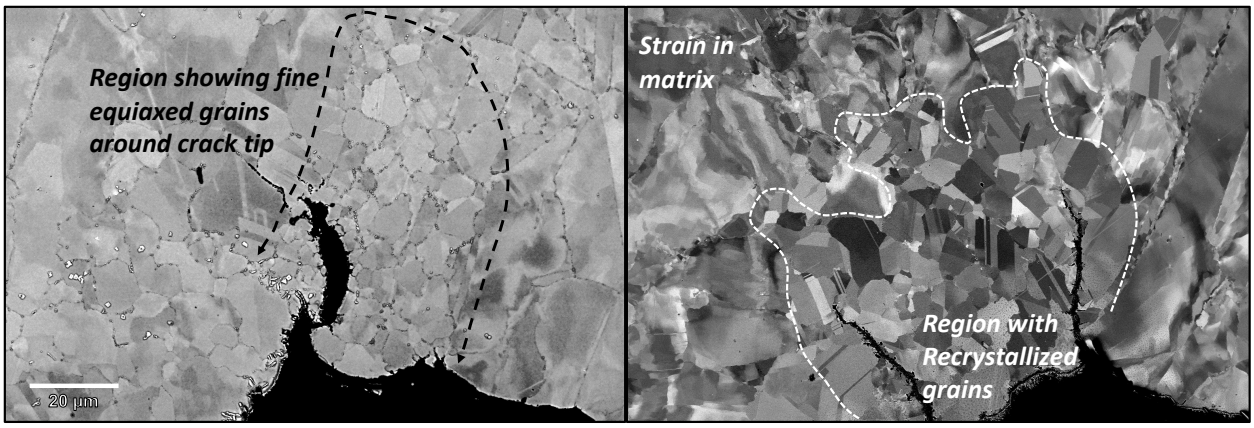

Figure 18. SEM image near weld toe showing a region of fine equiaxed (recrystallized) grains coincident with crack tip surrounded by strained grains in the matrix (channeling contrast)

DISCUSSION: FAILURE MECHANISM & LIKELY ROOT CAUSE(S)

Failure Mechanism

There are several potential cracking mechanisms which are known to cause weldability challenges in nickel-based alloys and specifically alloys of similar composition and structure to alloy 740H [6,7]. The observations in this work suggest that strain age cracking (SAC), also known as stress relief cracking (SRC) or stress relaxation cracking (SRxC), during the PWHT cycle is responsible for the observed cracking [8]. A summary of the supporting observations for SRxC are as follows:

1. *Timing:* The cracking likely occurred during the PWHT of the heater coil
    a. NDE inspections prior to PWHT did not identify any defects, but after PWHT 39 cracks or crack-like indications were identified from hydrostatic testing and PAUT inspection
    b. The cracks had a thin oxide scale suggesting cracking occurred early in the PWHT cycle
2. *Morphology*: The cracking is intergranular
    a. Crack initiation and growth was exclusively intergranular with minimal branching
    b. Isolated cavitation was observed ahead of some crack tips
    c. In all cases, a single main crack appeared to propagate rapidly, and its growth orientation did not follow a specific microstructural constituent (i.e., crack propagation was observed through base metal, HAZ, and weld metal).
3. *Stress State*: There is strong evidence for highly localized stresses leading to crack initiation
    a. Crack initiation was associated with a geometric stress concentration at the ID weld toe. Variable weld profiles showed some welds to have sharp corners and significant re-enforcement. These features are likely to promote stress localization leading to crack initiation. Through-wall crack growth was not associated with a unique weldment zone. Review of the literature, and similar observations for alloy 617, suggest that service induced SRxC (not from PWHT) in coal-fired superheater tubing shows very similar crack initiation and growth morphology [9].

b. Significant microstructural changes occurred in the HAZ/FL area near the weld toes:

   i. A small, recrystallized zone was observed near the crack initiation location. Recrystallization in the base metal can only occur if significant plastic strain was imparted prior to heat-treatment and subsequent heat-treatment relieves this stress through recrystallization and grain growth. At least two samples showed this specific feature.

   ii. Non-recrystallized grains in the same region showed channeling contrast in mixed electron imaging mode which supports the observation of an elevated level of strain within those grains.

   iii. Precipitate free zone (PFZ) and coarsened zones (CZ) were observed exclusively in this same region. This is the first time, to the authors' knowledge, that PFZs have been found in the base metal of an as-fabricated 740H welded structure. Previous research on PFZs and CZs in 740H focused on long-term creep exposures of 1,000's of hours and within compositional gradients typical for as-deposited weld metal [10]. For PFZ formation, a driving force for diffusion and a moving boundary needs to be present. The relaxation of highly localized residual stresses from the welding process is hypothesized to provide this driving force.

Other solid state cracking mechanisms such as weld solidification cracking and/or weld or HAZ liquation cracking are not plausible because the characteristics of these failure modes include cracking during the welding cycle (not uniquely associated with the PWHT aging heat-treatment), association of cracking with specific microstructural features such as grain boundaries in welds or HAZ, and evidence for low-melting point constituents which were not observed.

Potential Root Cause(s)

For SRxC to occur, three factors contribute to cracking: material susceptibility, thermal history, and stress state. The experience with alloy 740H in the STEP heater coil allows for a unique opportunity to understand the potential contributions of these factors and highlight the need for future research to better understand existing gaps.

- Material factors:
  - Alloy chemistry and microstructure (bulk and local) are known to influence SRxC susceptibility. For 740H, it has been shown that some heats of alloy 740H are more susceptible than others [11] but the specific chemistry factors have yet to be established. For the STEP heater, there were 24 unique heats of 740H tubing and cracking was linked to multiple heats. Thus, the data were inconclusive on the specific role of bulk chemistry. Additionally, there may exist a contribution to susceptibility from elements that may not be reported in traditional material test reports (MTRs) requiring independent chemical analysis to fully establish the metallurgical risk profile for the fabricated component.
  - Grain size has been shown to be an important factor in most solid-state cracking mechanisms in nickel-based alloys with larger grain heats generally possessing lower creep ductility and thus less able to accommodate the relaxation of stress by creep strain during the PWHT cycle [6]. However, in this work where there was a modest grain size difference in the same weld joint (see figure 15), the finer grain material showed cracking. This observation may suggest that grain size is not a dominant factor in the STEP heater cracking.

- Non-metallic inclusions, porosity, and other ‘hard’ microstructural features can provide crack initiation sites and reduced strain accommodation. In this analysis the typical carbide stringers in the base metal matrix did not contribute to the crack initiation or growth, and the welds were of high quality with no observable porosity or microcracking. Furthermore, the observed intergranular nature of the cracking compared to the intragranular distribution of such inclusion or carbide stringers makes the association of damage with these features impossible in a 2D plane.

- Thermal history
  - For this project, all the welds were performed using the manual GTAW process and required a multi-pass weld pass deposition to complete the weld. Thus, some variability in heat-input, interpass control, and overall process is expected. Examination of the overall weld quality, the lack of weld defects, and the successful welding of the header to stub tubes, may indicate that the welding process control is not contributing to the failure. For the available documentation it is impossible to determine if repeated stop-start locations, which may increase the number of local thermal histories, contribute to the observed pattern of damage in the affected tube-to-tube welds.
  - The PWHT for alloy 740H is not a ‘stress relief’ treatment. The purpose of the PWHT is to restore the strength of the weld metal and HAZ to that of the base metal through an age-hardening step. Review of the PWHT records and hardness testing of weldments indicated that the PWHT was conducted in accordance with the requirements in the Code Case (760 to 800^{o}C). Alternative PWHT temperatures are not currently permitted by Code Case 2702 but could be explored as selection of the PWHT is a balance between how rapidly the alloy age hardens (where there is generally a concomitant increase in strength and reduction in ductility) and how rapidly stresses are relieved.

- Stress state
  - While the welding process generally appears to be well controlled, the welding thermal cycle clearly had a pronounced effect on the tubular components of the STEP heater.
    - The fabrication sequence and design of the heater appears to be a significant factor in the application of manual welding of 740H. As shown in Figure 2, all header end welds were made on a table with good welder access. Additionally, all other header welds (flange, tube-to-header, endcap) were made with favorable access and positioning. Conversely, as shown in Figure 3, the welds made on the return end of the coil were more difficult for the welders to execute with restricted positioning and very limited access (especially for the final closure welds). It was also noted that since the return end was welded last, as overall flexibility decreased in the coil, some of the tubes had to be ‘jacked’ into place for welding. The result was highly variable weld profiles with excessive re-enforcement (even if within code limits) on the return end leading to the introduction of stress concentrations where cracking initiated. Tube circumferential weld modeling suggests that in some thinner-wall tubes the highest axial stress is present at the ID even without a geometric concentration [12]. Examination of Table 3 clearly shows that the return end had a cracking incidence of 4.5% compared to only 1.5% in the

header end. While the specific tube stress states are unknown, it is probable that stresses were generally higher in return end tubes than header end tubes.

- Welding residual stresses scale with local constraint that can be exacerbated by thickness or other geometric features so 'all things being equal' thicker welds would generally be considered to have higher residual stresses. Since the observed SRxCs were in tube-to-tube butt welds and not in the thicker section header welds, there are likely other factors to consider such as the specific weld geometry and welding practice (i.e., groove design, welding sequence, local constraint imposed by tube position). More careful inspection of Table 3 which breaks down the cracking by tube location and wall thickness, provides a series of interesting trends. For the header end, which did not experience significant cracking and where welder access was generally good, 6 of 9 the welds which did crack were in the thickest tubes. For the return end, cracking was not completely random, but the largest percentage of cracking occurred either in the thickest tubes or in the transition tubes where welding was used to transition from the 0.105 to 0.125-inch minimum wall thickness tubing. Furthermore, in these transition welds, the destructive evaluation showed cracking was always in the thicker tube in the transition (Figures 8 and 10 show 5 of the 6 welds examined from this transition region). Thus, it appears for similar geometry and welder access, the thicker tubes and/or thickness changes led to higher incidences of SRxC.

- Cold deformation (due to tube bending or improper machining practices) prior to welding can also lead to SRxC after welding. Based on the locations of failure, hardness profiles of welds, and general shop practices, this does not appear to be a contributing factor to the observed cracking.

In summary, while a full root cause analysis was not conducted, the observed failures (and observations from locations which did not experience cracking) from a well-controlled shop fabrication of the alloy 740H fired heater with >1,600 welds suggest variability in stress state was a significant factor in the observed damage. There was a clear bias in cracking to the return locations which had a combination of challenging/limited welder access, less flexibility (closure welds), and thickness transitions and/or thicker tubes. While alloy composition could not be conclusively ruled out as a factor, the grain size did not appear to contribute to the failure pattern. Welding and heat-treatment practices were controlled to specifications and are considered to be generally good industrial practice. Future, large-scale fabrication may consider alternative PWHT cycles and/or automated welding processes to allow for enhanced control over these variables.

Follow-on Activities

The failure investigation provided a unique set of learnings applicable to future installation(s) of alloy 740H and other nickel-based alloys susceptible to SRxC. Follow-on research to clarify the role of alloy chemistry and the mechanism for the formation of PFZs as well as additional advanced characterization of the failures will be beneficial to understanding mechanistic details. From a practical point of view, some of the key learnings for future applications were:

- Joint location and fabrication sequence should be considered in the design, especially in

regard to manual welding to provide ease of access and reduce local constraint and/or introduction of excessive welding residual stress

- Excessive reinforcement and other local, geometric changes that might otherwise be regarded as stress concentrations should be avoided or removed. Automated welding processes may help reduced the propensity for such features.
- Volumetric inspection must be performed after PWHT, and in addition to staged or limited inspection during or after welding, to ensure that the component or system is free of defects consistent with SRxC.

Future research topics which may lead to reduced propensity for SRxC include understanding the role of minor alloying elements, optimization of PWHT temperature and procedures, the use of alternative filler metals to control residual stresses, the effects of multi-pass welding and starting material heat-treatment condition, and determination of critical strain levels. EPRI, in cooperation with the U.S. DOE Solar Energy Technology Office, has recently launched a focused project to perform additional characterization of alloy 740H cracking and develop an industry guideline for use of 740H incorporating the lessons learned from this study and other failure investigations and industrial experience [13].

CONCLUSIONS

A gas-fired heater was designed and built to provide sCO2 at 715^{o}C and 255 bar at 100 kg/sec to the DOE STEP facility. The heater coil was the largest known application of an age-hardenable nickel-based alloy, alloy 740H, to ASME B&PV code construction. The fabrication involved welding procedure development, welder training, and the successful execution of over 1600 welds with a low initial weld failure rate (~1%). Following post-weld heat-treatment of the coil, the only welded connections which failed included ~3% of the tube-to-tube butt weld population. A comprehensive failure investigation was conducted to determine the failure mechanism and highlight factors contributing to root cause. In addition to review of the fabrication records and NDE (visual and volumetric) results, over 30 metallurgical mounts from 9 tubes were examined using a variety of metallographic techniques. The failure mechanism was determined to be stress relaxation cracking during the PWHT cycle (also known as strain age cracking or stress relief cracking). Cracking initiated on the ID of the tubes at the fusion line of the weld toes and propagated through the tube wall including base metal, fusion line, heat affected zone, and weld metal. The analysis suggests variability in stress state was a significant factor in the observed damage. There was a clear bias in return locations which had a combination of challenging/limited welder access, less flexibility (closure welds), and thickness transitions and/or thicker tubes. Alloy composition variations could not be conclusively ruled out as a factor in the failure, but general alloy structure and grain size did not appear to contribute to the failure. Welding and heat-treatment practices were controlled to specifications and are considered generally good industrial practice, but alternative PWHTs and/or automated welding processes were not considered which could enable more precise control on some of these variables.

Repairs were successfully completed on 39 welds and the heater has been shipped to site for final field erection. The application of 100% PAUT NDE provides the project a baseline for further in-service inspection after cyclic high-temperature operation of this first-of-a-kind heater. Lesson's learned are being applied to ongoing work with alloy 740H in the STEP project including the fabrication and installation of the interconnection piping. Follow-on research also continues focused on advanced characterization and development of industry guidelines for future application of alloy 740H in advanced energy systems and high-temperature conditions.

REFERENCES

[1] V. Bush. “GTI STEP forward on sCO2 Power.” *6th International sCO2 Power Cycles Symposium*, March 27-29, 2018, Pittsburgh, PA. http://sco2symposium.com/papers2018.shtml

[2] J. Marion et. al. “The STEP 10 MWe sCO2 Pilot Demonstration Status Update.” *ASME Turbo Expo 2020*: September 21-25, 2020 (Virtual). GT2020-14334. https://doi.org/10.1115/GT2020-14334

[3] M. Hauth, D. Stanley, D. Washburn. “ASME BPVC Code-Compliant Heater Design & Fabrication Using Inconel 740H.” *Proceedings – Evaluation of Welding Issues in High Nickel and Stainless Steel Alloys for Advanced Energy Systems.* DOE-NETL: March 10, 2021. https://netl.doe.gov/21WELD-proceedings

[4] 2021 ASME Boiler and Pressure Vessel Code, Section I: Rules for Construction of Power Boilers standard by ASME International © 2021.

[5] “Ni-25Cr-20Co Material, Case 2702-3.” Code Cases: Boiler and Pressure Vessels, Supplement 1. American Society of Mechanical Engineers © 2017.

[6] J. Dupont, J. C. Lippold and S. D. Keiser: ‘Welding metallurgy and weldability of nickel base superalloys’; 2009, New York, John Wiley and Sons Inc.

[7] S.A. David, J.A. Siefert, J.N. Dupont, J.P. Shingledecker. “Weldability and weld performance of candidate nickel base superalloys for advanced ultrasupercritical fossil power plants part I: fundamentals.” Science and Technology of Welding and Joining. Vol. 20, Issue 7 (October 2015), pp. 532-552.

[8] J. Siefert, J. Shingledecker, T. Lolla. “Power Generation Industry Experience.” Presentation at DOE sCO2 Cross-Cutting Team Workshop on: *Evaluation of Welding Issues in High Nickel and Stainless Steel Alloys for Advanced Energy Systems.* March 10, 2020.

[9] Simon Heckmann, Anne Woestmann, Ken Mitchell. “Recent Damage Evaluations on Austenitic Boiler Tubes associated with Supercritical Plant.” Presentation to EPRI – Program 87 Technology Transfer, Seattle, WA USA, June 18-19, 2018.

[10] Bechetti, D.H., Dupont, J.N., Watanabe, M. et al. Characterization of Discontinuous Coarsening Reaction Products in INCONEL® Alloy 740H® Fusion Welds. Metall Mater Trans A 48, 1727–1743 (2017). https://doi.org/10.1007/s11661-016-3952-2

[11] R. Kant, J. DuPont. “Stress Relief Cracking Susceptibility in High-Temperature Alloys.” *Welding Journal*, AWS, February 2019, 29-s. https://doi.org/10.29391/2019.98.003

[12] P. Dong. “On the Mechanics of Residual Stresses in Girth Welds.” *Journal of Pressure Vessel Technology.* Vol. 129, August 2007, © ASME. 345-354.

[13] *Innovative Method for Welding in Generation 3 CSP to Enable Reliable Manufacturing of Solar Receivers to withstand Daily Cycling at Temperatures Above 700°C.* DE-EE0009378

ACKNOWLEDGEMENTS

This research was supported by EPRI and the GTI-led STEP Demo supported by U.S. DOE Office of Fossil Energy DE- FE0028979. The authors wish to acknowledge Mary K. Havens, Kendall McCord, and Jay Richardson (EPRI) for their assistance with metallography and NDE. The assistance of Ronnie Golihue, Jack deBarbadillo, and Brian Baker of Special Metals and the engineering and fabrication teams and welders at Optimus is also acknowledged.